Traffic & Transportation

A Multi-Objective Dispatching Optimisation for Regional Bus Energy Saving

Yaqiong ZHANG[1], Yuguang WEI[2], Xinfeng YANG[3], Xu WU[4]

Original Scientific Paper
Submitted: 20 Dec 2024
Accepted: 4 Apr 2025

[1] 23115124@bjtu.edu.cn, School of Traffic and Transportation, Beijing Jiaotong University, Beijing, China
[2] ygwei@bjtu.edu.cn, School of Traffic and Transportation, Beijing Jiaotong University, Beijing, China
[3] xinfengyang@mail.lzjtu.cn, School of Traffic and Transportation, Lanzhou Jiaotong University, Lanzhou, China
[4] Corresponding author, wuxu@bjtu.edu.cn, School of Traffic and Transportation, Beijing Jiaotong University, Beijing, China

Publisher:
Faculty of Transport and Traffic Sciences, University of Zagreb

ABSTRACT
As energy conservation and sustainability become key priorities in public transportation, optimising bus scheduling with an emphasis on energy efficiency offers a practical pathway toward greener transit systems. However, existing studies often treat energy consumption and service quality in isolation, lacking an integrated framework for regional bus dispatch optimisation. This study proposes a multi-objective energy-saving dispatch model that jointly minimises passenger waiting time and vehicle energy consumption while considering vehicle allocation and passenger transfers. A vehicle-specific power (VSP)-based energy estimation method is introduced to enhance the accuracy of energy consumption assessments under real-world operating conditions. To solve the proposed model, we develop a two-phase optimisation algorithm that balances computational efficiency and solution quality. A case study on the Lanzhou regional transit network validates the model's feasibility, demonstrating improvements in both service levels and energy consumption. The findings contribute to the development of more sustainable and efficient regional bus scheduling strategies.

KEYWORDS
urban transport; energy saving dispatching; multi-objective optimisation; regional bus.

1. INTRODUCTION

Public transit plays a pivotal role in sustainable urban mobility, outperforming private vehicles in energy efficiency and environmental impact [1]. Studies indicate that optimised bus systems can reduce urban transport emissions by 18–22% compared to car-dominated travel patterns [2]. However, these environmental benefits heavily depend on operational factors, particularly vehicle occupancy rates. Data from the International Energy Agency (IEA) show that peak-hour bus occupancy ranges from 60% in Europe to 120% in Asia, while off-peak rates frequently drop below 15% [3]. When occupancy falls below 10–12%, life-cycle assessments reveal that buses lose their environmental advantage due to high embodied energy in manufacturing and low fuel utilisation rates [4]. This presents a key challenge: balancing service quality – frequency, comfort and reliability – with energy efficiency. Optimising vehicle allocation and operational planning is crucial to maintaining public transport's energy-saving benefits while enhancing its competitiveness and attractiveness.

Regional centralised scheduling is widely adopted in bus operations both domestically and internationally. This approach manages multiple routes within a specific area, enabling cross-line resource sharing and coordinated scheduling to improve efficiency [5]. Existing regional scheduling models primarily focus on

minimising passenger wait times [6] or maximising vehicle utilisation [7], often overlooking the trade-off between service quality and energy efficiency. For instance, Gkiotsalitis et al. found that increasing dispatch frequency reduces passenger delays by 30% but raises energy consumption by 15% when occupancy is suboptimal [8]. This underscores the need for integrated models that jointly optimise service quality and energy performance.

Given the interdependence between operational energy use and service performance, this study proposes a multi-objective optimisation framework for bus scheduling that simultaneously considers energy efficiency and service quality. We develop a novel two-phase solution algorithm capable of handling the nonlinear relationships between these competing objectives. The proposed method is validated using real-world data from Lanzhou's regional public transit network, which features a mix of bus rapid transit (BRT) and conventional buses operating in challenging terrain. Our results demonstrate measurable improvements in both energy efficiency and passenger service metrics, providing valuable insights for transit agencies seeking to balance environmental and operational performance.

This study makes three key contributions. (1) A unified modelling framework that captures the interdependence between energy consumption and service quality in bus operations. (2) An efficient computational approach for solving the resulting multi-objective optimisation problem. (3) Empirical validation through a real-world case study, demonstrating the practical applicability and benefits of the proposed method.

The remainder of this paper is structured as follows: Chapter 2 provides a literature review. Chapter 3 introduces the quantitative index of energy consumption. Chapter 4 proposes the energy-saving dispatching model, with Section 4.1 defining the mathematical notations and Sections 4.2 and 4.3 analysing bus operational characteristics and formulating the multi-objective optimisation model, respectively. Chapter 5 presents the NSGA-II algorithm along with a comprehensive weighting method. Chapter 6 discusses the case study, including optimised results and sensitivity analysis. Finally, Chapter 7 concludes this paper.

2. LITERATURE REVIEW

At the regional level of bus scheduling optimisation, numerous studies have explored strategies to enhance both transit efficiency and service quality. Wei et al. developed a two-layer optimisation model that minimises bus purchase costs and exhaust emissions, promoting both economic and environmental sustainability [9]. Building on this, Lee et al. introduced reliability indicators and time-space networks, refining operational schedules by incorporating fixed time windows and accounting for uncertain passenger flow conditions [10].

Further advancing scheduling methodologies, Silva-Soto et al. focused on the time synchronisation of bus arrivals at overlapping stops. They formulated a mixed-integer optimisation model based on time-index variables and employed an improved genetic algorithm to enhance solution efficiency [11]. In a different approach, Zhu et al. examined public transport management strategies during disruptions, proposing a boarding limit strategy to ensure equitable passenger access under capacity constraints, such as during pandemics [12]. They also developed a reservation-based bus scheduling approach using a mixed-integer nonlinear programming (MINLP) model to address travel time uncertainty while optimising both passenger wait times and operational efficiency [13].

In recent years, dynamic scheduling approaches for high-frequency bus lines have gained increasing attention. Chen et al. proposed a novel bi-modal traffic control framework that integrates bus frequency optimisation with perimeter control through a three-dimensional passenger macroscopic fundamental diagram (3D-pMFD). Their passenger-oriented strategy regulates both private vehicle flows and public transit operations at the network level, significantly enhancing regional mobility efficiency [14]. In a similar vein, Gkiotsalitis and van Berkum developed a rolling-horizon optimisation model using convex programming to maintain service regularity and minimise passenger waiting times while ensuring computational efficiency. However, real-world operational constraints often necessitate more advanced techniques, such as heuristic algorithms or MINLP, to tackle scheduling complexities [15].

Beyond scheduling, traffic management strategies also play a crucial role in improving transit sustainability. Naseri et al. explored the impact of high-occupancy vehicle (HOV) lanes on urban freeway congestion. Their simulation-based study of the Tehran-Karaj corridor demonstrated that HOV lanes can effectively alleviate congestion, providing policy-relevant strategies that may also benefit bus priority systems and transit-oriented development [16]. This underscores the need for an integrated approach that combines vehicle-level efficiency improvements with system-level traffic management to enhance public transportation sustainability.

Although much energy efficiency research has focused on road-based transit, similar principles apply across various transportation and energy systems. For instance, Ghalebzade et al. examined axle load distribution in railway networks using Simpack, modelling articulated trains with hydraulic actuators. Their findings, which comply with EN14363/UIC518 standards, identified risks in curved track navigation and proposed a control method to mitigate axle load disparity in intercity trains, offering insights relevant to urban transit vehicle energy efficiency [17].

Moreover, energy efficiency considerations extend beyond conventional fuel consumption models to broader transport and mobility systems. Asemi et al. studied working fluid selection in Stirling refrigerators, showing that helium provides superior cooling capacity at optimal pressure compared to air. Although focused on cryogenic applications, this research highlights the significance of thermodynamic optimisation in energy management, a principle that is also relevant to electric bus battery cooling and efficiency [18]. Similarly, Rahim et al. conducted a lifecycle analysis of hybrid energy storage systems (HESS) for electric vehicles, revealing that ultracapacitor integration can significantly extend battery lifespan, reducing long-term costs despite a higher initial investment. Their findings provide valuable insights for the sustainable electrification of transit systems [19].

Despite extensive research on bus scheduling and energy efficiency, existing approaches often fail to integrate both objectives within a unified framework. Our approach incorporates real-world operational constraints and nonlinear interactions, ensuring practical applicability. The proposed framework is validated using empirical data from Lanzhou's transit network, demonstrating its potential to enhance both service efficiency and sustainability.

3. BUSES ENERGY CONSUMPTION ANALYSIS

Consistent with the findings of Song et al. [20], who validated VSP as a more reliable energy predictor compared to speed and acceleration, *Figure 1* illustrates the VSP-based calculation process, which includes:

— VSP bin classification;
— Bin-specific energy coefficients;
— Energy consumption factor.

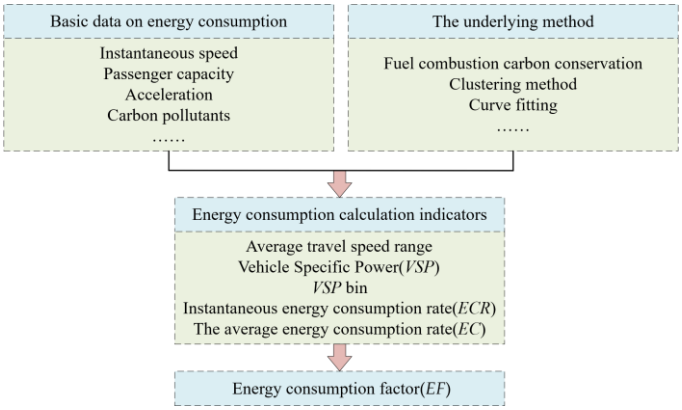

Figure 1 – The calculation framework of energy consumption

1) Vehicle specific power (VSP)

VSP (kw/kg) is the instantaneous output power of a motor vehicle per unit mass [20], as *Equation 1*:

$$VSP = v(a \cdot (1+\varepsilon) + g \cdot i + g \cdot C_R) + \frac{0.5\rho \cdot C_D \cdot A \cdot v^3}{(n \cdot m + M)} \quad (1)$$

where v denotes the speed, a refers to the acceleration, i is the road slope and take $i = 0$, g is the gravitational acceleration and take $g = 9.8m/s^2$, $C_R$is the rolling resistance coefficient, ρ refers to the air density and take $\rho = 1.2kg/m^3$, A and M respectively represent the maximum frontal cross-sectional area of the vehicle and the unladen mass of the vehicle, m is the average weight of passengers, taking 65.

2) Instantaneous energy consumption (ECR)

$ECR(g \cdot s^{-1})$ refers to the amount of energy consumed by a motor vehicle per second [20]. According to the principle of carbon conservation of fuel combustion, the exhaust emission data of automobiles are converted into energy consumption rate, as shown in *Equation 2*:

$$ECR = (ER_{CO_2} \cdot \frac{12}{44} + ER_{CO} \cdot \frac{12}{28} + ER_{HC} \cdot \frac{12}{13}) \cdot \frac{1}{C\%} \quad (2)$$

where ER_{CO_2}, ER_{CO} and ER_{HC} are the emission rates of CO_2, CO and HC, respectively. $C\%$ is the mass ratio of carbon in the fuel, which is 0.86 for diesel and 0.45 for natural gas.

3) Average energy consumption (EC)
Affected by changes in the traffic environment or the vehicle performance, the energy consumption corresponding to the same VSP value has a large dispersion [21]. In this paper's case, the instantaneous energy consumption rate is clustered at intervals of 1 kw/kg, so $ECR(g \cdot s^{-1})$ of y VSP bin is obtained as *Equation 3*:

$$EC_y = \frac{\sum_y ECR_y}{n_y} \quad (3)$$

where n_y is the total time of the y VSP bin.

4) Energy consumption factor (EF)
There is a good normal distribution fitting law between the VSP distribution of the vehicle and the average travel speed, which can be effectively used for the energy consumption calculation of motor vehicles. In this paper's case, the average speed of 60 consecutive pieces of second-by-second data is used as the average travel speed. $EF_{v_k}(g \cdot km^{-1})$ of the k speed interval can be expressed by *Equation 4*:

$$EF_{v_k} = \frac{3600 \cdot \sum_y EC_y \cdot Fr_{y,k}}{v_k} \quad (4)$$

$$Fr_{y,k} = \frac{T_{y,k}}{T_k} \quad (5)$$

where $v_k(km \cdot h^{-1})$ is the average travel speed of the speed interval. $Fr_{y,k}$ indicates the percentage of the y VSP bin when speed interval is k, as *Equation 5*, T_k and $T_{y,k}$ are the total time of the k speed interval and the y VSP bin.

4. MODEL OF REGIONAL BUS ENERGY SAVING DISPATCHING

Following standard practice in transit modelling [22], we assume no vehicle overtaking occurs, as is typical in high-frequency systems where headway adherence is prioritised over overtaking. This aligns with our study system's dispatch policies. Passenger arrivals are modelled as uniform within headways, a widely used assumption for short headways (<10–15 min) supported by empirical studies [23].

4.1 Notations

In order to describe the running state of public transport vehicles on the road network, the variable symbols and relevant parameters are set in *Tables 1* and *2*.

Table 1 – Variables

Variables	Meanings
$f_{b_l^i}$	The departure time of bus b_l^i from the parking lot s_l^0, decision variable, and the other decision variable is the vehicle type, which can be described by $q_{b_l^i}$
$d_{b_l^i,s_l^j}$	The arrival time of bus b_l^i at station s_l^j
$w_{b_l^i,s_l^j}$	The dwell time of bus b_l^i at station s_l^j
$z_{b_l^i,s_l^j}$	The stranded passengers who are unable to take the bus b_l^i
$h_{b_l^i,s_l^j}$	The total passengers who are waiting for bus b_l^i at station s_l^j
$A_{b_l^i,s_l^j}$	The actual number of boarding passengers
$D_{b_l^i,s_l^j}$	The actual number of alighting passengers
$C_{b_l^i,s_l^j}$	The number of passengers on bus b_l^i upon leaving the station s_l^j

Table 2 – Parameters

Parameters	Meanings
l	Line index, $l \in L, L = \{l \mid l = 1,2,3,\ldots,N\}$, N is the number of regional lines
i	Vehicle index
j	Station index, $j \in S$, S is the set of regional bus stations, $S = \{S_l \mid l \in L\}$
S_l	The station set of the line l, $S_l = \{s_l^0, s_l^1, \ldots, s_l^{m_l}\}$, m_l is the number of the stations, and s_l^0 is parking depot
s_l^j	The No. jth station of the line l, $s_l^j \in S_l$
S_t	The transfer station set, $S_t = \left\{(s_{l_1}^p, s_{l_2}^q) \middle\| s_{l_1}^p, s_{l_2}^q \in S, l_1, l_2 \in L\right\}$
B_l	The bus set of the line l, $B_l = \{b_l^1, b_l^2, \ldots, b_l^i, \ldots, b_l^{n_l}\}$, denotes t and n_l is the number of departures in the hypothetical time frame
b_l^i	The No. ith bus of the line l, $b_l^i \in B_l$
$\alpha_{s_l^j}$	Passenger alighting rate of station s_l^j, which refers to the proportion of the number of passengers off to all passengers on the bus
$\beta_{s_l^j}$	Arrival rate of station s_l^j, which to the number of passengers arriving per unit time (1 min)
$tr_{s_{l_1}^p, s_{l_2}^q}$	Passenger transfer rate of station $s_{l_1}^p$ of bus line l_1 to station $s_{l_2}^q$ of bus line l_2
$t_{s_l^{j-1}, s_l^j}$	The travel time between stations s_l^{j-1} and s_l^j
$q_{b_l^i}$	The capacity of bus b_l^i
T_1 *and* T_2	The scheduling time window
t_{min} *and* t_{max}	The minimum and maximum departure intervals

4.2 Dynamic analysis of bus operation

Affected by the decision variables departure time and vehicle type, there are four types of auxiliary variables through the dynamic analysis of bus operation.

Dwell time

The bus's dwell time is the sum of the platform passenger service time, the bus start-stop and bus's doors opening or closing time, of which the service time for passengers is the greater time taken by passengers to get on or off, as represented in *Equation 6*.

$$w_{b_l^i, s_l^j} = t_1 + t_2 \cdot max\left\{A_{b_l^i, s_l^j}, D_{b_l^i, s_l^j}\right\} \tag{6}$$

where t_1 is the time for the bus to stop-start and open or close the door, t_2 is the average time taken by passengers to get on and off. According to research statistics, the bus opening and closing time is about 1–3 s, the entry and stopping time is about 4–8 s, the departure start time is 6–15 s, the average boarding time per passenger is 2.6–3 s, the average getting off time is 1.7–2s, so set $t_1 = 0.27\ min$ and $t_2 = 0.06\ min$.

Arrival time

The arrival time is divided into two categories: the arrival time at the departure station and the arrival time at non-departure stations. The difference is that the arrival time at non-origin stations includes the stop time at the previous station.

$$d_{b_l^i,s_l^1} = f_{b_l^i} + t_{s_l^0,s_l^1} \tag{7}$$

The arrival time of the non-departure station is the sum of its arrival time at the previous station, the dwell time at the front station and the travel time between stations.

$$d_{b_l^i,s_l^j} = d_{b_l^i,s_l^{j-1}} + w_{b_l^i,s_l^{j-1}} + t_{s_l^{j-1},s_l^j} \tag{8}$$

Number of passengers alighting or boarding

The actual number of alighting passengers is the product of the number of passengers on the bus and the alighting rate, which can be calculated by the following equation.

$$D_{b_l^i,s_l^j} = \alpha_{b_l^i,s_l^j} \cdot C_{b_l^i,s_l^{j-1}} \tag{9}$$

The number of passengers boarding is the lesser of the number of remaining seats and waiting passengers, as in *Equation 10*, in which the number of remaining seats is the rated capacity minus the number of people on board when the vehicle leaves the previous station, plus the number of people getting off the bus.

$$A_{b_l^i,s_l^j} = min\left\{h_{b_l^i,s_l^j}, Q_{b_l^i} - C_{b_l^i,s_l^{j-1}} + D_{b_l^i,s_l^j}\right\} \tag{10}$$

The number of waiting persons consists of three groups: the number of new passengers within the headway, the number of passengers stranded and the number of passengers who transfer to this bus.

$$h_{b_l^i,s_l^j} = (d_{b_l^i,s_l^j} - d_{b_l^{i-1},s_l^j}) \cdot \beta_{b_l^i,s_l^j} + z_{b_l^{i-1},s_l^j} + D_{b_{l_1}^i,s_{l_1}^j} \cdot tr_{s_{l_1}^j,s_l^i} \tag{11}$$

The number of passengers on the bus

The number of passengers on the bus refers to the passengers' number after the bus left the station, so as to station j, which is the number of passengers on the bus from $j-1$ station minus the number of people getting off at the station, plus the number of people boarding the station, as follows segmentation in *Equation 12*:

$$C_{b_l^i,s_l^j} = \begin{cases} 0, & j = 0 \\ C_{b_l^i,s_l^{j-1}} - D_{b_l^i,s_l^j} + A_{b_l^i,s_l^j}, & j \in \{1,2,\dots m_l\} \end{cases} \tag{12}$$

where $j = 0$ indicates that the bus departs from the depot with no passengers on board.

4.3 The multi-objective optimisation model

Passengers waiting time

It is assumed that passenger arrivals follow a uniform distribution, meaning that the waiting time for new arrivals is half of the headway. Passengers who experience delays at the stop will have to wait for the next bus, as shown in *Figure 2*.

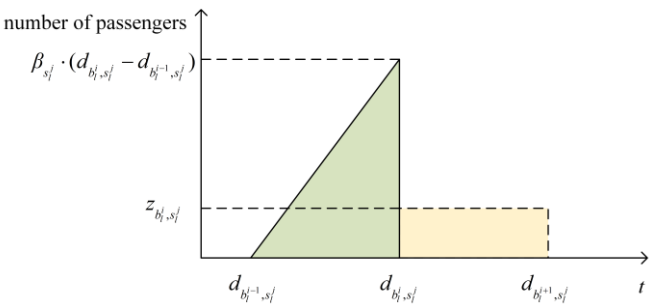

Figure 2 – New arrivals and stranded passengers waiting time

Regional bus transfer refers to the process in which passengers switch between different bus routes, typically at transportation hubs or interchange points. The passenger transfer waiting time is defined as the difference between the departure time of the target transfer bus and the time the passenger arrives at the transfer station, as illustrated in *Figure 3*.

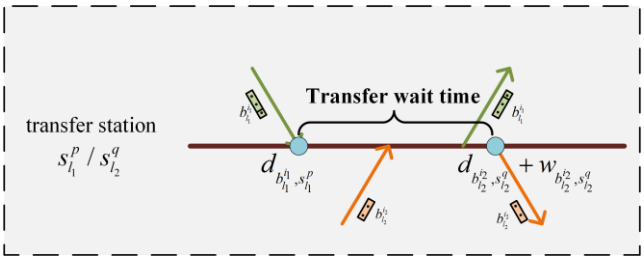

Figure 3 – Waiting time for transfer passengers

Considering all platforms and vehicles in the area, the total waiting time of passengers can be obtained by accumulating the waiting time of passengers at all bus stops. The minimum total waiting time is the objective to meet passenger demand, as shown in *Equation 13*:

$$min\, z_1 = \sum_{i=1}^{n_l}\sum_{j=1}^{m_l}\sum_{l\in L}\left[\frac{(d_{b_l^i,s_l^j} - d_{b_l^{j-1},s_l^j})^2 \cdot \beta_{b_l^i,s_l^j}}{2} + (d_{b_l^{i+1},s_l^j} - d_{b_l^i,s_l^j}) \cdot z_{b_l^i,s_l^j}\right] + \sum_{i_1=1}^{n_{l_1}}\sum_{i_2=1}^{n_{l_2}}\sum_{l_1、l_2\in L}\sum_{s_{l_1}^p、s_{l_2}^q\in s_t} D_{b_{l_1}^{i_1},s_{l_1}^p} \cdot tr_{s_{l_1}^p,s_{l_2}^q}(d_{b_{l_2}^{i_2},s_{l_2}^q} + w_{b_{l_2}^{i_2},s_{l_2}^q} - d_{b_{l_1}^{i_1},s_{l_1}^p}) \tag{13}$$

Buses energy consumption

The energy consumption calculation method is the product of the energy consumption factor corresponding to each speed interval and it is travelled distance, and the total energy consumption is the sum of the energy consumption of all buses in the scheduling time window. The minimum energy consumption is the objective to meet the energy saving dimension, as shown in *Equation 14*:

$$min\, z_2 = \sum_{i=1}^{n_l}\sum_{l\in L}\frac{(d_{s_l^{m_l},b_l^i} - f_{b_l^i}) \cdot \sum_{k=1} EF_{v_k,b_l^i} \cdot F_{v_k,b_l^i}}{1000} \tag{14}$$

where F_{v_k,b_l^i} is the running distance of the bus in the speed interval.

Average load factor rate constraint

To quantify passenger comfort levels, we evaluate the bus load factor (defined as the ratio of actual passenger count to vehicle capacity). Higher load factors indicate greater crowding, which directly reduces passenger comfort. Following the widely adopted classification [5], we categorise comfort levels into five distinct tiers based on load factor thresholds, as detailed in *Table 3*.

Table 3 – Passenger comfort level and load factor correspondence

Comfort	A	B	C	D	E
Load factor rate	<50%	50%-80%	80%-100%	100%-110%	>110%

In order to meet the passenger travel demand and comfort requirements during peak hours, the constraints are set as *Formula 15*:

$$\alpha \le \frac{\sum_{j=1}^{m_l} C_{b_l^j,s_l^j}}{(m_l - 1) \cdot q_{b_l^i}} \le \beta \tag{15}$$

Departure reliability constraint

The coefficient of variation of the headway reflects the relative fluctuations of bus services [23], which can be expressed as the ratio of the standard deviation of the headway to the mean, as *Formula 16*:

$$\frac{\sqrt{\frac{1}{n_l-1}\sum_{i=1}^{n_l}\left[\left(f_{b_l^i}-f_{b_l^{i-1}}\right)-\overline{HW_l}\right]^2}}{\overline{HW_l}} \le \gamma \tag{16}$$

where $\overline{HW_l}$ represents the average of the time headway of all vehicles sent out on the line during the time window, the calculation method is as follows:

$$\overline{HW_l} = \frac{\sum_{i=1}^{n_l}\left(f_{b_l^i}-f_{b_l^{i-1}}\right)}{n_l} \tag{17}$$

where n_l is the total number of departures in that time window.

In addition, *Formulas 18* and *19* are time window constraints and departure interval constraints, respectively.

$$T_1 \le f_{b_l^i} \le T_2, i = 1,2,\ldots,n_l, l \in L \tag{18}$$

$$t_{min} \le f_{b_l^i} - f_{b_l^{i-1}} \le t_{max}, i = 2,\ldots,n_l, l \in L \tag{19}$$

Then, the overall optimisation model of regional bus dispatching is established as *Equations 13–19*.

5. TWO-PHASE ALGORITHM

To resolve the fundamental trade-off between energy consumption minimisation and passenger waiting time reduction, we developed a two-stage optimisation framework (*Figure 4)*:

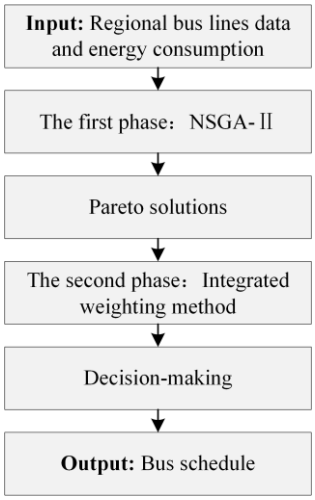

Figure 4 – The two-phase algorithm flow

(1) Pareto solutions generation

The NSGA-II algorithm, designed for multi-objective optimisation, identifies non-dominated solutions through three key mechanisms: non-dominated sorting to prioritise solution quality, adaptive mutation to maintain diversity and crowding distance computation to ensure a well-distributed Pareto front.

$CH_d = (ch_1, ch_2, \ldots, ch_N)$ is designed as the basic structure of chromosomes, where N is the number of regional bus lines. $ch_l = (f_l, q_l)$ represents a pair of interrelated genes, $f_l = (f_{b_l^1}, f_{b_l^2}, \ldots, f_{b_l^{n_l}})$ denotes the departure time of each bus on line l and $q_l = (q_{b_l^1}, q_{b_l^2}, \ldots, q_{b_l^{n_l}})$ indicates the corresponding capacity of each bus. N genes are linked to form a chromosome.

Based on the structure of the chromosomes, to ensure that the mutated chromosomes directly satisfy the time window and departure interval constraints, the mutation strategy includes four cases.

1) Adjust the vehicle capacity

The operation applied to genes q_l. Randomly select s elements from the gene q_l and change its capacity. The mutation process is shown in *Figure 5*.

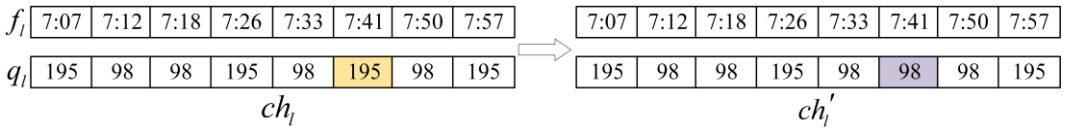

Figure 5 – The first mutation operator

2) Optimise the departure time

The operation applied to genes f_l. Randomly generate a mutation point ρ, and generate a random integer u_1 that obeys a uniform distribution $u(t_{min}, t_{max})$, and let $f_{b_l^\rho} = f_{b_l^{\rho-1}} + u_1$, which can be divided into three cases:

a) If $f_{b_l^\rho} - f_{b_l^{\rho-1}} \in [t_{min},\ t_{max}]$, there is no need to change the genes in other positions, and just replace the mutation point gene with the mutated gene, as shown in *Figure 6*.

b) If the vehicles b_l^ρ and $b_l^{\rho+1}$ do not meet the departure interval constraint, the chromosome initialisation operation is repeated from this mutation point onward, as shown in *Figure 7*.

c) If the newly generated departure time after mutation exceeds the time window constraint, this element is removed, as shown in *Figure 8*.

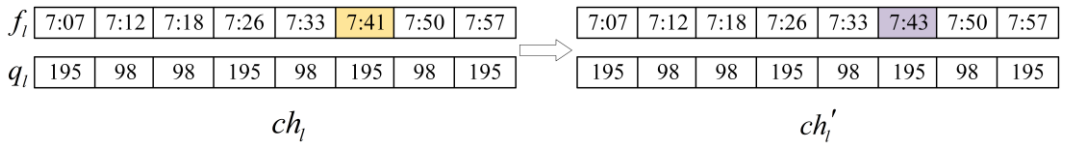

Figure 6 – The second mutation operator for case a

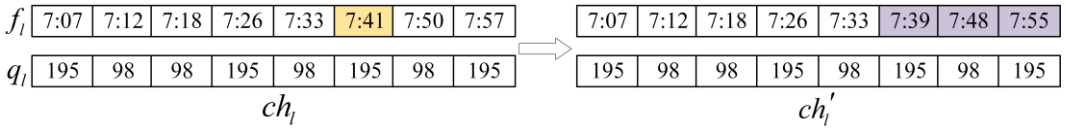

Figure 7 – The second mutation operator for case b

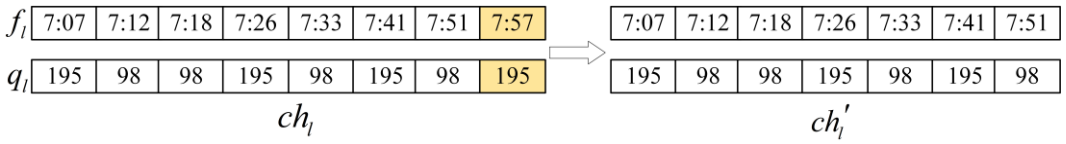

Figure 8 – The second mutation operator for case c

(2) Decision-making phase

In the integrated weighting method, we employ the entropy method [9] for objective weighting to quantify the inherent information utility of each indicator. For subjective weighting, we adopt a multi-criteria decision-making (MCDM) approach [10], with the number of departures selected as the primary criterion based on operational priorities.

Table 4 – The corresponding table of departure frequency and subjective weight

Departure frequency	**5-6**	**6-7**	**7-8**	**8-9**	**9-10**	**10-11**
u_1 (weight)	0.7	0.6	0.5	0.4	0.3	0.2
u_2 (weight)	0.3	0.4	0.5	0.6	0.7	0.8

6. CASE ANALYSIS

6.1 Data preparation

Regional bus lines

The study covers five bus lines (a total of 85 stations) in Lanzhou, with operational data derived from historical statistics. *Figure 9* illustrates the network schematic, where l_1 denotes the BRT corridor and others represent conventional routes. All vehicles are CNG-powered buses, with technical specifications detailed in *Table 5*. Transfer relationships between lines are documented in *Table 6*, while *Table 7* summarises station characteristics and operational parameters collected through field surveys. The simulation evaluates the morning peak (7:00–8:00) with departure intervals constrained to 3–10 minutes.

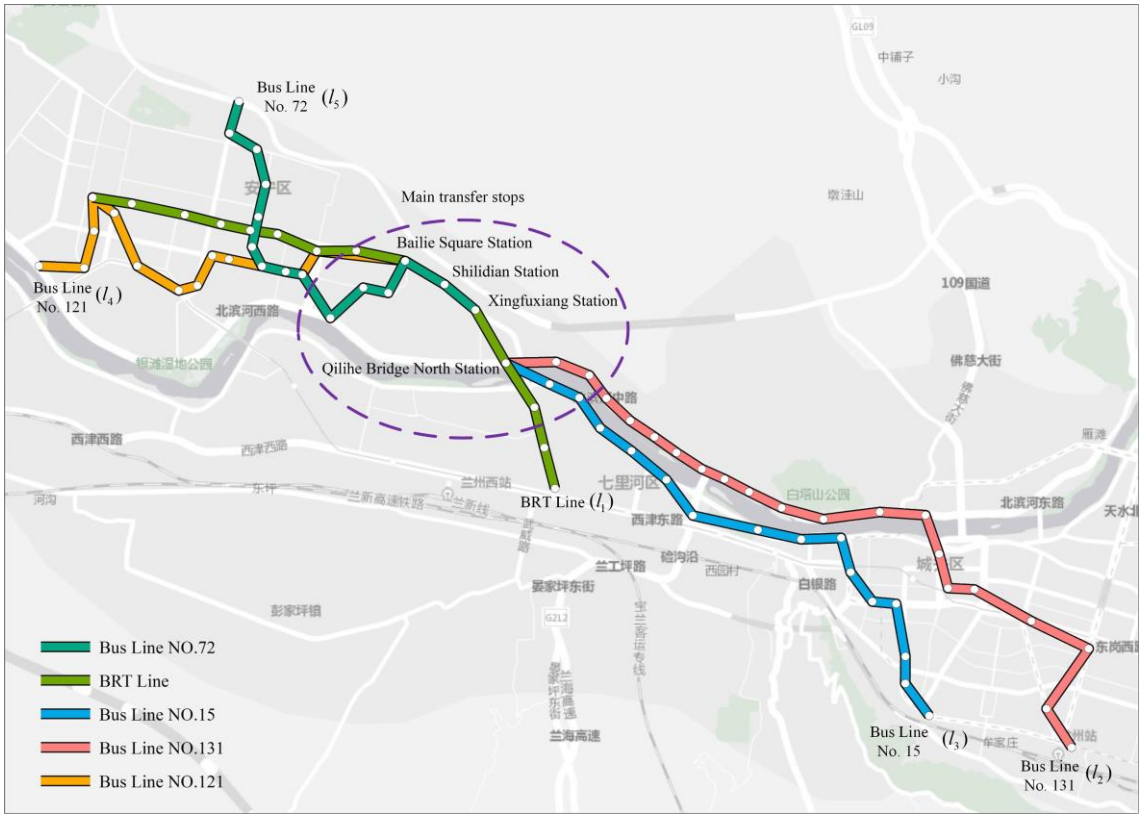

Figure 9 – Regional bus lines in Lanzhou

Table 5 – Information on bus lines and vehicles

Bus lines	l_1	l_2	l_3	l_4	l_5
The full length of the line /(km)	9.1	16.3	11.7	8.6	6.8
Types of buses	12/18m BRT	NBT	NBT	NBT	NBT
Curb weight M /(kg)	11200/17850	11700	11700	11700	11700
A /(m^2)	7.78/8.16	7.78	7.78	7.78	7.78
C_R	0.00917	0.00938	0.00938	0.00938	0.00938
Rated passenger capacity	98/195	96	96	96	96

Notes: The rated passenger capacity is measured in persons. BRT system utilises articulated buses, while the normal bus transit (NBT) employs single-deck buses as its fleet composition.

Table 6 – The basic transfer relationship of regional bus lines

Bus lines	Transfer station	Transfer rate	Bus lines	Transfer station	Transfer rate	Bus lines	Transfer station	Transfer rate
$l_1 - l_2$	$s_{l_1}^9 - s_{l_2}^1$	0.01	$l_1 - l_4$	$s_{l_4}^{13} - s_{l_1}^{11}$	0.04	$l_2 - l_5$	$s_{l_5}^{15} - s_{l_2}^3$	0.02
	$s_{l_1}^{10} - s_{l_2}^2$	0.03	$l_1 - l_5$	$s_{l_5}^{13} - s_{l_1}^9$	0.08	$l_3 - l_4$	$s_{l_4}^{11} - s_{l_3}^1$	0.2
	$s_{l_1}^{11} - s_{l_2}^3$	0.10		$s_{l_5}^{14} - s_{l_1}^{10}$	0.05		$s_{l_4}^{12} - s_{l_3}^2$	0.05
$l_1 - l_3$	$s_{l_1}^9 - s_{l_3}^1$	0.15		$s_{l_5}^{15} - s_{l_1}^{11}$	0.03		$s_{l_4}^{13} - s_{l_3}^3$	0.02
	$s_{l_1}^{10} - s_{l_3}^2$	0.05	$l_2 - l_4$	$s_{l_4}^{11} - s_{l_2}^1$	0.1	$l_3 - l_5$	$s_{l_5}^{13} - s_{l_3}^1$	0.15
	$s_{l_1}^{11} - s_{l_3}^3$	0.03		$s_{l_4}^{12} - s_{l_2}^2$	0.05		$s_{l_5}^{14} - s_{l_3}^2$	0.05
	$s_{l_1}^{12} - s_{l_3}^4$	0.02		$s_{l_4}^{13} - s_{l_2}^3$	0.03		$s_{l_5}^{15} - s_{l_3}^3$	0.03
$l_1 - l_4$	$s_{l_4}^{11} - s_{l_1}^9$	0.15	$l_2 - l_5$	$s_{l_5}^{13} - s_{l_2}^1$	0.07	—	—	—
	$s_{l_4}^{12} - s_{l_1}^{10}$	0.06		$s_{l_5}^{14} - s_{l_2}^2$	0.04	—	—	—

Table 7 – The basic operating parameters of bus stops

l	s_l^j	$t_{s_l^{j-1},s_l^j}$	$\beta_{s_l^j}$	$\alpha_{s_l^j}$	l	s_l^j	$t_{s_l^{j-1},s_l^j}$	$\beta_{s_l^j}$	$\alpha_{s_l^j}$	l	s_l^j	$t_{s_l^{j-1},s_l^j}$	$\beta_{s_l^j}$	$\alpha_{s_l^j}$	l	s_l^j	$t_{s_l^{j-1},s_l^j}$	$\beta_{s_l^j}$	$\alpha_{s_l^j}$
l_1	$s_{l_1}^1$	1	6	0.0	l_2	$s_{l_2}^7$	1	1	0.10	l_3	$s_{l_3}^4$	3	2	0.1	l_4	$s_{l_4}^7$	2	2	0.1
	$s_{l_1}^2$	1	1	0.03		$s_{l_2}^8$	1	2	0.07		$s_{l_3}^5$	3	1	0.08		$s_{l_4}^8$	1.1	1	0.35
	$s_{l_1}^3$	1.75	6	0.04		$s_{l_2}^9$	1	1	0.03		$s_{l_3}^6$	2	1	0.05		$s_{l_4}^9$	2	1	0.2
	$s_{l_1}^4$	1	7	0.05		$s_{l_2}^{10}$	1.5	1	0.06		$s_{l_3}^7$	1.7	3	0.1		$s_{l_4}^{10}$	3.5	2	0.15
	$s_{l_1}^5$	1	2	0.13		$s_{l_2}^{11}$	1	1	0.10		$s_{l_3}^8$	2.9	1	0.15		$s_{l_4}^{11}$	2	1	0.6
	$s_{l_1}^6$	1	3	0.11		$s_{l_2}^{12}$	1.25	1	0.15		$s_{l_3}^9$	3	1	0.2		$s_{l_4}^{12}$	3.5	0	1
	$s_{l_1}^7$	1.5	6	0.07		$s_{l_2}^{13}$	1	2	0.30		$s_{l_3}^{10}$	3	2	0.05	l_5	$s_{l_5}^1$	1	6	0
	$s_{l_1}^8$	1.8	5	0.30		$s_{l_2}^{14}$	1	2	0.20		$s_{l_3}^{11}$	1.8	1	0.35		$s_{l_5}^2$	2	3	0.05
	$s_{l_1}^9$	1.4	8	0.35		$s_{l_2}^{15}$	1.75	1	0.40		$s_{l_3}^{12}$	4.6	1	0.15		$s_{l_5}^3$	1.5	4	0.1
	$s_{l_1}^{10}$	1.2	5	0.40		$s_{l_2}^{16}$	2	3	0.15		$s_{l_3}^{13}$	2.1	1	0.5		$s_{l_5}^4$	1	2	0.1
	$s_{l_1}^{11}$	1.8	4	0.30		$s_{l_2}^{17}$	1	1	0.07		$s_{l_3}^{14}$	1.3	1	0.65		$s_{l_5}^5$	1	3	0.2
	$s_{l_1}^{12}$	1.7	2	0.25		$s_{l_2}^{18}$	2.5	1	0.08		$s_{l_3}^{15}$	2	2	0.1		$s_{l_5}^6$	1.5	2	0.15
	$s_{l_1}^{13}$	2.8	1	0.09		$s_{l_2}^{19}$	1.2	1	0.1		$s_{l_3}^{16}$	3	1	0.3		$s_{l_5}^7$	1.25	1	0.2
	$s_{l_1}^{14}$	1.9	0	0.15		$s_{l_2}^{20}$	1.3	0	0.1		$s_{l_3}^{17}$	2	0	0.4		$s_{l_5}^8$	2	1	0.35
	$s_{l_1}^{15}$	2.2	0	1		$s_{l_2}^{21}$	5	1	0.08		$s_{l_3}^{18}$	1.5	0	1		$s_{l_5}^9$	1	2	0.25
l_2	$s_{l_2}^1$	1	7	0		$s_{l_2}^{22}$	3	0	0.12	l_4	$s_{l_4}^1$	1.5	4	0		$s_{l_5}^{10}$	1	2	0.15
	$s_{l_2}^2$	1.5	3	0		$s_{l_2}^{23}$	4.5	0	0.15		$s_{l_4}^2$	2	3	0.05		$s_{l_5}^{11}$	1	1	0.2
	$s_{l_2}^3$	3	4	0.02		$s_{l_2}^{24}$	1.5	0	1		$s_{l_4}^3$	1	5	0.1		$s_{l_5}^{12}$	2	1	0.25
	$s_{l_2}^4$	1	2	0.03	l_3	$s_{l_3}^1$	2.5	5	0		$s_{l_4}^4$	2	3	0.15		$s_{l_5}^{13}$	1	1	0.3
	$s_{l_2}^5$	1	2	0.06		$s_{l_3}^2$	2	4	0.04		$s_{l_4}^5$	1.2	1	0.2		$s_{l_5}^{14}$	3	1	0.4
	$s_{l_2}^6$	1.75	1	0.05		$s_{l_3}^3$	3.5	3	0.08		$s_{l_4}^6$	1.3	2	0.25		$s_{l_5}^{15}$	2	0	1

Energy consumption calculation

The experimental data were obtained from bus performance monitoring studies. The study fleet comprised three vehicle types: 12-metre BRT buses, 18-metre articulated BRT buses and conventional Yutong ZK6125HNG2 city buses – all utilising compressed natural gas (CNG) propulsion. *Figure 10* presents the morning peak (7:00–8:00) speed distribution analysis, where:

— No. denotes the bus line identifier;
— Speed values represent 60-second rolling averages of instantaneous measurements.

The average energy consumption rate and energy consumption factor were calculated using *Equations (1)–(5)*. Corresponding characteristic curves were generated through MATLAB simulations, including

— *Figure 11a*: VSP versus average energy consumption rate;
— *Figure 11b*: Speed range versus energy consumption factor.

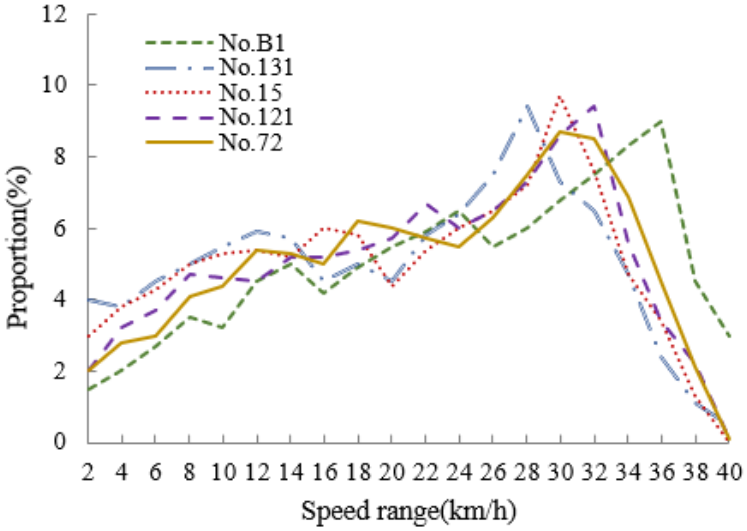

Figure 10 – Speed distribution of buses

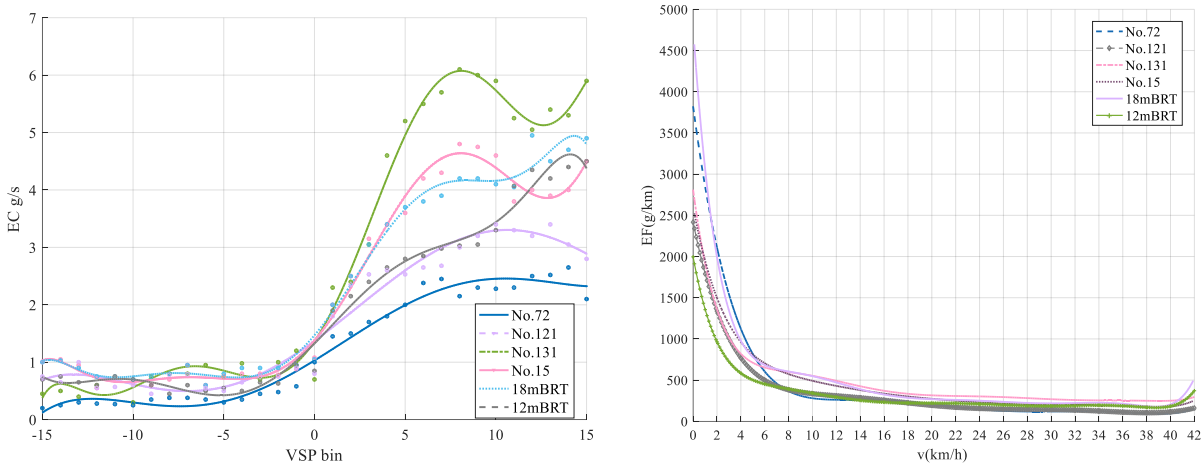

(a) *(b)*

Figure 11 – a) VSP versus average energy consumption rate; b) Speed range versus energy consumption factor

6.2 Analysis of results

Optimised results

The Transit Capacity and Quality of Service Manual (TCQSM) [6] classifies bus service reliability levels based on headway variation, where a coefficient of variation (CV) below 0.3 indicates "excellent" reliability. For our case study, we set the load factor threshold at 0.8–1.0 to balance fuel efficiency and service quality. Using the NSGA-II algorithm with parameters (population size $SN = 50$, crossover probability $P_c = 0.5$ and mutation probability $P_m = 0.3$), we obtained the Pareto frontier shown in *Figure 12*.

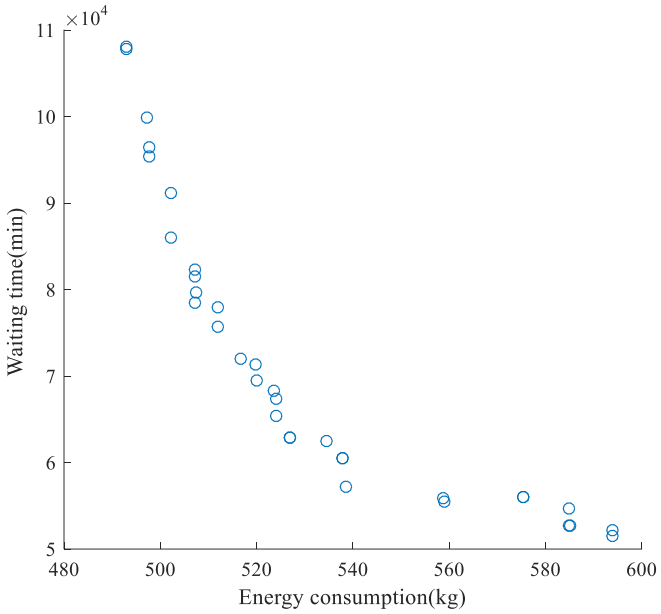

Figure 12 – The distribution of Pareto solutions

The Pareto solutions and their corresponding comprehensive objective values are presented in *Table 8*. *Figure 13* illustrates the scheduling scheme (Scheme 1) derived from the optimisation. For comparative analysis, we evaluated Scheme 1 against a uniform interval dispatch (UID) schedule, maintaining the same number of departures. The service level comparison between energy-saving dispatch (ESD) and UID is summarised in *Table 9*.

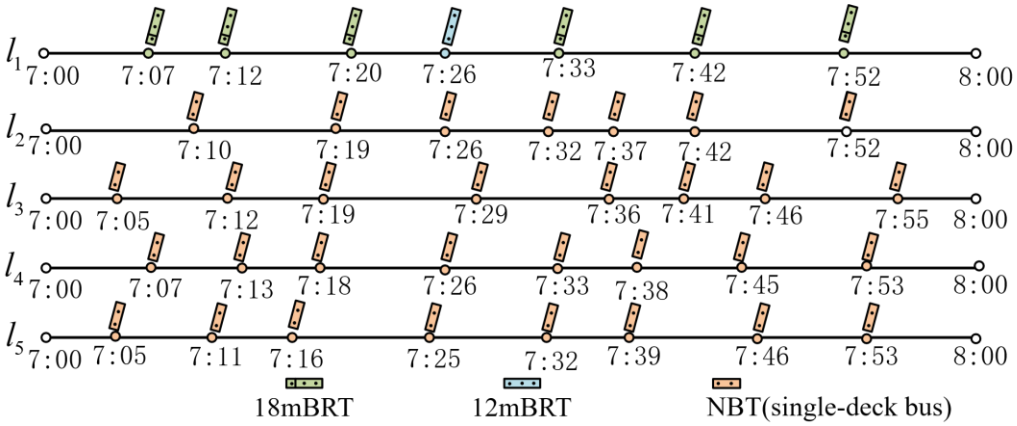

Figure 13 – Vehicle operation schedules for Scheme 1

Table 8 – The Pareto solutions with higher synthesised objective values

Scheme	Wait time (min)	Energy consumption (kg)	The number of departures	Synthesised objective values
1	51477.14	593.9	38	0.701
2	52160.63	593.8	38	0.701
3	54753.39	585.0	38	0.692
4	52687.49	585.1	38	0.691
5	55921.59	558.8	36	0.663
6	55485.39	558.9	36	0.663
7	42508.14	659.2	42	0.662
8	45478.90	657.2	42	0.662
9	47681.19	640.2	41	0.648
10	47214.35	640.3	41	0.647

Table 9 – Comparison of service level and energy consumption across bus lines

Bus line	Wait time (min)		Energy consumption (kg)		Maximum load factor		Departure reliability	
	ESD	UID	ESD	UID	ESD	UID	ESD	UID
1	14172.7	25144.8	112.8	114.1	1.02	1.13	0.23	0
2	15568.4	18434.8	156.1	156.4	0.98	0.98	0.29	0
3	9696.5	9786.7	165.2	165.6	0.99	0.99	0.27	0
4	4861.3	5577.9	83.1	83.6	0.85	0.80	0.17	0
5	7178.1	7299.1	76.7	77.6	0.95	1.05	0.20	0
Total	51477	54673.3	593.9	597.3	—	—	—	—

Based on the case study results, the following key conclusions can be drawn:

1) Energy-saving scheduling scheme and passenger waiting time: The optimised energy-saving scheduling scheme reduces passenger waiting time by adjusting departure intervals and rationally allocating vehicle types. This is due to the better alignment of vehicle capacity with passenger demand, which minimises unnecessary waiting time and optimises resource utilisation. The reduction in waiting time implies that the scheduling adjustments are effectively matching the peak demand periods, leading to more efficient operations.
2) Energy consumption reduction: The reduction in operational energy consumption is a direct result of balancing the load factor across the buses within the time window. By adjusting the departure intervals and vehicle types, the energy-efficient allocation ensures that buses are operating closer to their optimal capacity, avoiding the excess energy consumption that occurs with underutilised vehicles.
3) Load factor and passenger comfort: The decrease in the maximum load factor indicates that the optimised scheduling scheme leads to more evenly distributed passengers across buses, reducing overcrowding and improving comfort. This result suggests that by spreading passenger demand more evenly, the system can enhance the travel experience for passengers, especially during peak periods.

Sensitivity analyses

The bus scheduling plan is not a single solution but a set of solutions, offering a certain degree of flexibility in selection. Therefore, the sensitivity analyses of energy costs and vehicle capacity are conducted based on the distribution of the Pareto solution set. The energy cost coefficient is set to half and twice its original value, while vehicle capacity is increased and decreased by 20% of its original value. The resulting Pareto solution distributions are shown in *Figure 14*.

For energy consumption costs, the distribution of Pareto solutions across the three scenarios remains consistent, which can be attributed to the influence of the non-dominated sorting algorithm. By computing the integrated objective values of the Pareto solutions using the second-stage algorithm, we observe that lower energy costs lead to top-ranked solutions with shorter passenger waiting times, emphasising social welfare. Conversely, higher energy costs shift the preference toward minimising operational costs.

The sensitivity analysis of vehicle models reveals that when the vehicle capacity is reduced by approximately 20%, the solutions outperform those with the original capacity. However, when the vehicle capacity is increased by 20%, the solutions are similar to those with the current capacity. This analysis can provide valuable insights for decision-makers during vehicle procurement.

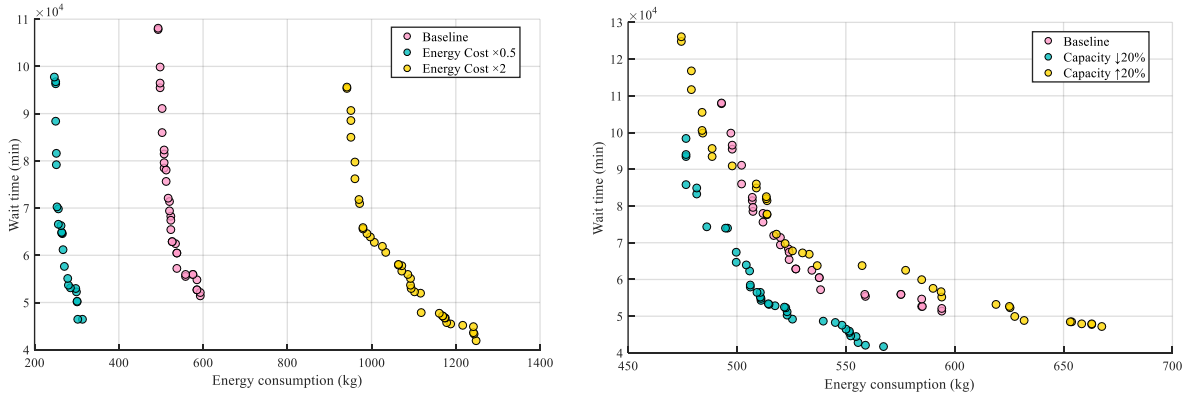

(a) *(b)*

Figure 14 – a) Different energy cost Pareto solutions; b) Different vehicle capacity Pareto solutions

7. CONCLUSION

An effective departure strategy is crucial for achieving energy-efficient bus scheduling from an operational management perspective. This study develops a VSP-based energy consumption estimation method, integrating key factors such as speed, passenger load and vehicle type to improve the accuracy of energy consumption assessment. Based on this method, we propose a multi-objective regional bus scheduling model that optimises both passenger waiting time and vehicle energy consumption, while considering practical constraints such as time windows, departure intervals, load factors and service reliability.

To effectively solve the proposed scheduling model, we design a two-phase optimisation framework. The first phase employs NSGA-II to generate a Pareto-optimal solution set, ensuring a balance between energy efficiency and service quality. The second phase applies an integrated weighting method to facilitate decision-making and refine the final scheduling plan.

A case study based on Lanzhou's regional bus network demonstrates the feasibility and effectiveness of the proposed model and algorithm. The results indicate that optimising variable departure intervals and vehicle type allocation plays a crucial role in enhancing both energy efficiency and service performance. Compared to traditional fixed-interval scheduling, the proposed approach achieves a more sustainable and efficient regional public transport system.

However, flexible vehicle scheduling increases labour costs for bus crews, and the sensitivity analysis in this paper indicates that excessively high energy costs can alter the priority of scheduling schemes. Our model does not account for the profitability of the bus company but instead focuses solely on maximising social welfare and environmental benefits. Future research on energy-saving scheduling should further explore how to balance these factors with economic benefits.

ACKNOWLEDGEMENTS

The research was supported by the Fundamental Research Funds for the Central Universities (No. 2024JBZX036).

REFERENCES

[1] Andrei A, et al. Driving towards sustainable transportation systems: A bottom-up traffic modal choices analysis using responsible management for future development planning. *Promet-Traffic & Transportation*. 2024;36(4):593-607. DOI: 10.7307/ptt.v36i4.556.

[2] Chester M, Horvath A. Environmental assessment of passenger transportation should include infrastructure and supply chains. *Environmental Research Letters*, 2009;4(2):024008. DOI: 10.1088/1748-9326/4/2/024008.

[3] International Energy Agency. *Global EV Outlook 2022* [Internet]. Paris: IEA; 2022. Available from: https://www.iea.org/reports/global-ev-outlook-2022

[4] Spielmann M, et al. Life cycle assessment of public transport services. *The International Journal of Life Cycle Assessment*, 2007;12(1):43-49. DOI: 10.1065/lca2006.12.292.

[5] Yang X, Qi Y. Research on optimization of multi-objective regional public transportation scheduling. *Algorithms*. 2021;14(4). DOI: 10.3390/a14040108.

[6] Ruiz M, Segui-Pons JM, Mateu-Lladó J. Improving bus service levels and social equity through bus frequency modelling. *Journal of Transport Geography*. 2017;58:220-233. DOI: 10.1016/j.jtrangeo.2016.12.005.

[7] Ceder A. Public-transport vehicle scheduling with multi vehicle type. *Transportation Research Part C: Emerging Technologies*. 2011;19(3):485-497. DOI: 10.2139/ssrn.4908074.

[8] Gkiotsalitis K, Cats O. Public transport planning adaption under the COVID-19 pandemic crisis: Literature review of research needs and directions. *Transport Reviews*, 2021;41(3):374-392. DOI: 10.1080/01441647.2020.1857886.

[9] Wei M, Sun B. Bi-level programming model for multi-modal regional bus timetable and vehicle dispatch with stochastic travel time. *Cluster Computing*. 2017;20(1):401-411. DOI: 10.1007/s10586-016-0719-x.

[10] Lee E, Cen X, Lo HK. Scheduling zonal-based flexible bus service under dynamic stochastic demand and Time-dependent travel time. *Transportation Research Part E: Logistics and Transportation Review*. 2022;168. DOI: 10.1061/9780784481523.057.

[11] Silva-Soto YI, Ibarra-Rojas OJ. Timetabling with flexible frequencies to synchronise groups of bus lines at common stops. *Transportmetrica A: Transport Science*. 2020;17(4):978-1001. DOI: 10.1080/23249935.2020.1822952.

[12] Zhu C, et al. Joint optimization of bus scheduling and seat allocation for reservation-based travel. *Transportation Research Part C: Emerging Technologies*. 2024(163):104631.DOI: 10.1016/j.trc.2024.104631.

[13] Zhu C, et al. Designing boarding limit strategy by considering stop-level fairness amid the COVID-19 outbreak. *Transportmetrica A Transport Science*. 2024;20(2):2167500. DOI: 10.1080/23249935.2023.2167500.

[14] Chen S, et al. Passenger-oriented traffic management integrating perimeter control and regional bus service frequency setting using 3D-pMFD. *Transportation Research Part C: Emerging Technologies*. 2022;135:103529. DOI: 10.1016/j.trc.2021.103529.

[15] Gkiotsalitis K, van Berkum EC. An exact method for the bus dispatching problem in rolling horizons. *Transportation Research Part C: Emerging Technologies*, 2020;110:143-165. DOI: 10.1016/j.trc.2019.11.009.

[16] Naseri A, et al. Simulating the performance of HOV lanes for optimal urban traffic management. *Transportation Research Interdisciplinary Perspectives*. 2024;23:101010. DOI: 10.1016/j.trip.2023.101010.

[17] Ghalebzade F, et al. Analyzing operational dynamics: Centralized load distribution and suspended wagons in self-propelled trains. *Advanced Control for Applications: Engineering and Industrial Systems*. 2024;6:e236. DOI: 10.1002/adc2.236.

[18] Asemi H, Daneshgar S, Zahed R. Experimental investigation of gamma Stirling refrigerator to convert thermal to cooling energy utilizing different gases. *Future Technology*. 2023;2(2):1-10. DOI: 10.55670/fpll.futech.2.2.1.

[19] Rahim R, Pourezzat AA, Jafari M. Hybrid energy storage system for electric motorcycles: Technical and economic analysis. *Case Studies in Thermal Engineering*. 2024;60:104613. DOI: 10.1016/j.csite.2024.104613.

[20] Song G, Yu L. Estimation of fuel efficiency of road traffic by characterization of vehicle-specific power and speed based on floating car data. *Transportation Research Record: Journal of the Transportation Research Board*. 2009;2139(1):11-20. DOI: 10.3141/2139-02.

[21] Perugu H. Emission modelling of light-duty vehicles in India using the revamped VSP-based MOVES model: The case study of Hyderabad. *Transportation Research Part D: Transport and Environment*. 2019;68:150-163. DOI: 10.1016/j.trd.2018.01.031.

[22] Chen D, He J, Lin S, Yang Z. Passenger arrival patterns and its implications for bus operation: The impact of schedule reading behavior on average waiting times at bus stops. *Transport Policy*.2025;163:310-322. DOI: 10.1016/j.tranpol.2025.01.021.

[23] Jesper BI, et al. Passenger arrival and waiting time distributions dependent on train service frequency and station characteristics: A smart card data analysis. *Transportation Research Part C: Emerging Technologies*. 2018;90:292-306. DOI: 10.1016/j.trc.2018.03.006.